LETTER

doi:10.1038/nature11474

Near-infrared background anisotropies from diffuse intrahalo light of galaxies

Asantha Cooray[1], Joseph Smidt[1], Francesco De Bernardis[1], Yan Gong[1], Daniel Stern[2], Matthew L. N. Ashby[3], Peter R. Eisenhardt[2], Christopher C. Frazer[1], Anthony H. Gonzalez[4], Christopher S. Kochanek[5], Szymon Kozłowski[5,6] & Edward L. Wright[7]

Unresolved anisotropies of the cosmic near-infrared background radiation are expected to have contributions from the earliest galaxies during the epoch of reionization[1–5] and from faint, dwarf galaxies at intermediate redshifts[6,7]. Previous measurements[8–12] were unable to pinpoint conclusively the dominant origin because they did not sample spatial scales that were sufficiently large to distinguish between these two possibilities. Here we report a measurement of the anisotropy power spectrum from subarcminute to one-degree angular scales, and find the clustering amplitude to be larger than predicted by the models based on the two existing explanations. As the shot-noise level of the power spectrum is consistent with that expected from faint galaxies, a new source population on the sky is not necessary to explain the observations. However, a physical mechanism that increases the clustering amplitude is needed. Motivated by recent results related to the extended stellar light profile in dark-matter haloes[13–15], we consider the possibility that the fluctuations originate from intrahalo stars of all galaxies. We find that the measured power spectrum can be explained by an intrahalo light fraction of 0.07 to 0.2 per cent relative to the total luminosity in dark-matter haloes of 10^9 to 10^{12} solar masses at redshifts of about 1 to 4.

To distinguish between the two interpretations of the near-infrared anisotropy power spectrum, we have analysed imaging data from the Spitzer Deep, Wide-Field Survey (SDWFS)[16]. This survey covers 10.5 square degrees on the sky with the IRAC instrument in its four bands between 3.6 and 8 μm. We focus on the data at 3.6 and 4.5 μm, as the confusion from zodiacal light limits extragalactic background studies at 5 and 8 μm (ref. 8). The data were taken in four separate epochs between 2004 and 2008, and observations were conducted in ways to minimize the systematic errors associated with anisotropy measurements. In particular, the four different epochs were observed at different roll angles of the instrument so that the measurements are robust against detector artefacts, persistence resulting from saturated bright stars, and variations in the bias level. The SDWFS mapping strategy was also optimized to facilitate self-calibration[17] of the data by maximizing inter-pixel correlations.

To limit the influence of bright stars and galaxies, including extended sources, in our anisotropy measurements, we mask all sources that are detected either in the combined SDWFS data or in the ancillary multi-band optical and near-infrared data[18]. The effects of assembling ('mosaicing') individual detector frames, pixelization of the maps, and the detected-source mask are captured by the map-making transfer function (Supplementary Information). We compute the transfer function and its uncertainty with a large set of sky simulations. The point-spread function (PSF) and its uncertainty were determined by measuring and modelling the PSF of stars in different subregions of the image and computing the variance of the differences between the modelled PSFs.

The power spectrum measurements at 3.6 and 4.5 μm show a clear excess above the shot-noise level (Fig. 1). The shot noise dominates the anisotropy power spectrum at subarcminute angular scales corresponding to angular multipole moment $\ell > 10^5$. Such a shot noise is expected from the small-scale Poisson behaviour of the spatial distribution of sources on the sky. The clustering amplitude we measure at $\ell \approx 10^4$ is fully consistent with existing measurements of the anisotropy power spectrum with IRAC in deeper, but smaller-area, fields[8,9,12]. At angular scales of tens of arcseconds, corresponding to $\ell > 5 \times 10^4$, our shot-noise level is higher than that of a recent measurement by a factor of about 2 because deeper data allow more of the fainter sources to be individually detected and masked[12]. Nevertheless, we independently confirm the near-infrared background anisotropies at angular scales larger than a few arcminutes at the previously reported amplitude[12].

The near-infrared anisotropies have been previously interpreted as either due to spatial clustering of primordial galaxies responsible for cosmic reionization[8] or due to faint, dwarf galaxies at low redshifts that fall below the individual source detection threshold of Spitzer images[6,7,9]. Figure 1 shows that the measured fluctuations in SDWFS are well above both these interpretations. The power spectrum predictions for galaxies at redshifts $z > 6$ rely on a combination of analytical calculations[19] and numerical simulations[20] of reionization. If we force the $z > 6$ galaxy model to fit the power spectrum data, then the integrated intensity of $z > 6$ galaxies is about 2 nW m^{-2} sr^{-1} at 3.6 μm (ref. 19). To reach such a high intensity, these galaxies must be very efficient in converting baryons to stars[20]. In fact, the required star-formation rate conflicts with the measured metal abundance at $z > 4$, the measured X-ray background when compared to X-rays from stellar end products such as black holes, and the measured luminosity functions of bright Lyman-dropout galaxies[21]. Unless a significant revision of our current understanding of $z > 6$ galaxy statistics is made, it is unlikely that the measured anisotropy power spectrum is dominated by the primordial galaxies.

A large compilation of multi-wavelength luminosity functions and galaxy number counts[7] allow predictions to be made for the intensity fluctuations due to low-redshift, faint galaxies. The measured luminosity-function slope at the faint end is used to extrapolate to the fainter galaxies that are undetected in the Spitzer images. An increase in the faint-end slope above the measured values does not increase the clustering amplitude on the angular scales of interest without modifying the shot-noise level. Although the clustering amplitude is smaller than the measurements, the prediction related to faint, dwarf galaxies[7] shows that they generate a shot-noise level consistent with the measured small-scale anisotropy power spectrum (Fig. 1). At angular scales of a few tens of arcminutes, the measurements are such that the clustering amplitude is a factor of about 6 to 10 above the prediction. Although this difference suggests that a new model to explain the anisotropy power spectrum is clearly needed, the consistency with the shot-noise level is

[1]Department of Physics and Astronomy, University of California, Irvine, California 92697, USA. [2]Jet Propulsion Laboratory, California Institute of Technology, Pasadena, California 91109, USA. [3]Harvard-Smithsonian Center for Astrophysics, 60 Garden Street, Cambridge, Massachusetts 02138, USA. [4]Department of Astronomy, University of Florida, Gainesville, Florida 32611, USA. [5]Department of Astronomy, The Ohio State University, Columbus, Ohio 43210, USA. [6]Warsaw University Observatory, Aleje Ujazdowskie 4, 00-478 Warszawa, Poland. [7]Department of Physics and Astronomy, University of California, Los Angeles, California 90095, USA.

such that we do not need to invoke a new population of point sources on the sky to explain the observations.

While keeping the shot-noise level the same, the measurements can be explained by any physical effect that boosts the two-halo term of the halo model of galaxy clustering[22]. One possibility is to increase the halo masses of the faint, dwarf galaxies so that their clustering amplitude is increased with a corresponding increase in their large-scale bias factor[22].

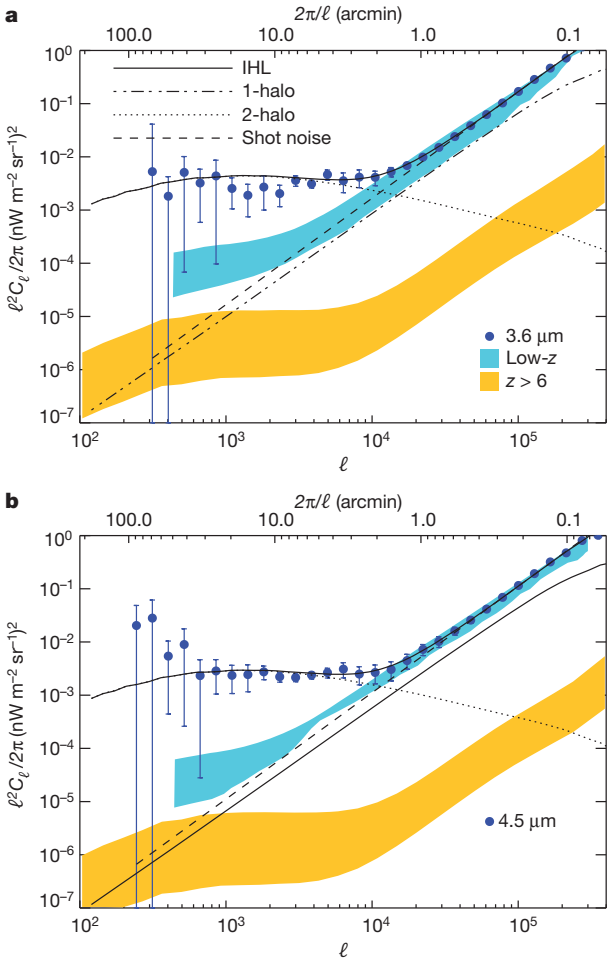

Figure 1 | The angular power spectrum of the unresolved near-infrared background. Shown is the total power spectrum $\ell^2 C_\ell/2\pi$ of SDWFS at 3.6 μm (**a**) and 4.5 μm (**b**) as a function of the multipole moment ℓ. The corresponding angular scale $2\pi/\ell$ is listed on the upper x axis in units of arcminutes. SDWFS imaging data were taken on the same field at four separate epochs in January 2004, August 2007, February 2008 and March 2008. Each epoch of data, taken over 7 to 10 days, includes 4,300–4,900 IRAC frames that were combined to make mosaics using the self-calibration algorithm[17]. The total integration time is 6 min per pixel. These individual frames were first visually inspected and cleaned of artefacts such as asteroidal trails and hot pixels. Through cross-correlations between sum and difference maps between epochs, we make independent measurements of the sky signal and noise. The final power spectrum (filled circles) is the average of the multi-epoch cross-correlation data under the assumption that the instrumental noise is not correlated between epochs. The two shaded regions show the expected contribution from $z > 6$ galaxies[19] (blue) and low-redshift galaxies[7] (yellow) based on two model predictions in the literature. The lines shows a diffuse IHL model where we show the signal in terms of the total (solid), one (dashed-dotted) and two (dotted) halo terms. The dashed line is the best-fit shot-noise signal that dominates the anisotropies at small angular scales. In **a** and **b**, the error bars are 1σ uncertainties in the power spectrum. They are determined by propagating the errors from the beam measurement into the power spectrum, while the simulations, based out of noise measurements, were used to obtain instrumental and sky variance. The quadratic sum of these errors and the map-making transfer function uncertainty constitutes the final error estimate.

The required modification needed to explain the fluctuation data is, however, ruled out by the measured number counts and the redshift distribution[7]. Because intensity anisotropies are measured, another option is to introduce a luminosity component to the dark-matter haloes that remain unmasked when the hosted bright galactic disks are masked as part of the analysis. Such a possibility exists in the literature in the form of diffuse halo stars in the extended stellar profile of galaxies out to distances of 100 kpc (ref. 23). In our anisotropy measurements, we mask the faintest detected galaxies to 3–4 arcsec, which removes the light from the bulges and disks of those galaxies. To remove the diffuse light component, we would have to mask to a radius greater than 10 arcsec around each galaxy. The surface density of galaxies down to AB-magnitude $m_{AB} < 22$ at 3.6 μm is such that we expect 2 to 3 galaxies within a circle of radius 10 arcsec. Thus masks which successfully remove the diffuse component leave no pixels on the map from which to measure the anisotropy power spectrum.

Existing studies discuss this extended emission in terms of the diffuse intrahalo light (IHL)[15], explained as originating in tidally stripped stars produced during galaxy mergers and collisions. The fraction of stripped stars is expected to be a function of the halo mass, with more massive haloes containing a larger fraction of the diffuse halo emission[13,14,24]. On galaxy cluster scales, the diffuse intracluster light[25,26] is a significant

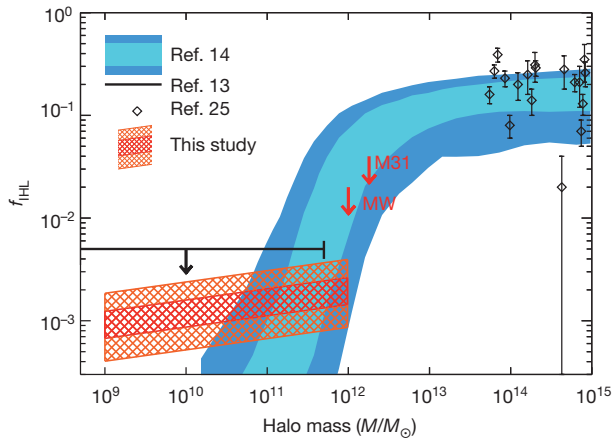

Figure 2 | The IHL fraction from diffuse stars as a function of the halo mass. The dark and light blue shaded regions show the 95% and 68% range of intrahalo light fraction f_{IHL} relative to the total luminosity of the dark-matter haloes as a function of the halo mass M from an analytical prediction[14], valid for $f_{IHL} > 4 \times 10^{-4}$ and $M > 5 \times 10^{10}\ M_\odot$ and at $z = 0$. We show the case where dark matter subhaloes on orbits passing within a critical radius of the host halo centre contribute their light to the central galaxy rather than to the diffuse component. We also show a prediction where f_{IHL} is constant[13], due to dwarf galaxies that are completely destroyed, with a value of ~0.005 when $M \lesssim 5 \times 10^{11}\ M_\odot$ (solid line fixed at $f_{IHL} = 5 \times 10^{-3}$). The downward arrow indicates the possibility that the constant f_{IHL} value for low-mass haloes may be smaller at higher redshifts. The red and orange hatched regions at the bottom of the plot are the preferred 68% and 95% confidence level range, respectively, on f_{IHL} from our analysis of the SDWFS near-infrared anisotropy power spectrum. The mass range is determined by the minimum and maximum halo masses consistent with the halo model fit that includes the IHL component. Both the mass and f_{IHL} ranges are valid over the broad redshift interval from $z = 1$ to 4 over which the anisotropy signal is generated. We do not find a significant halo mass dependence on the IHL fraction, with the mass-dependent power-law having a value of 0.09 ± 0.01 between 10^9 and $10^{12}\ M_\odot$ (see Supplementary Information section 9), consistent with the possibility that f_{IHL} is mass independent[13] when $M \lesssim 5 \times 10^{11}\ M_\odot$. Our model requires the total luminosity/halo-mass relation to evolve with redshift as $(1+z)^{1.2 \pm 0.1}$. This luminosity evolution with redshift can also be absorbed into the evolution of $f_{IHL}(M)$ with redshift. For reference, we also show measurements (open diamonds) and 1σ errors of the intracluster light[26], the galaxy group and cluster analogue for IHL when $M > 5 \times 10^{13}\ M_\odot$. At halo masses around $10^{12}\ M_\odot$ we show (red arrows) the 95% confidence level upper limit on f_{IHL} estimated for Milky Way[29] and Andromeda (M31)[30].

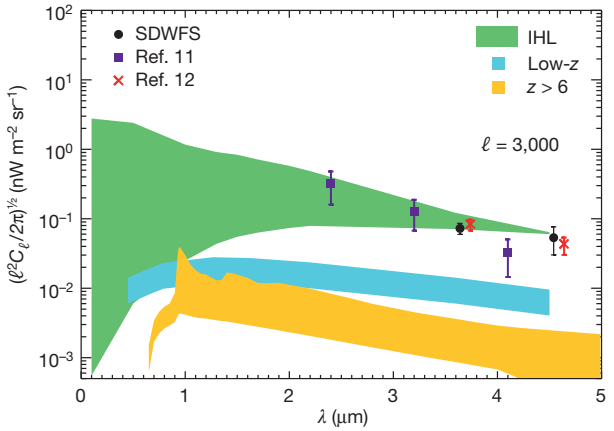

Figure 3 | The spectral energy distribution of infrared background anisotropies. Data symbols show the frequency spectrum of near-infrared and optical background anisotropies as a function of the wavelength. We show the r.m.s. fluctuation amplitude at $\ell = 3{,}000$, corresponding to fluctuations at 6-arcminute angular scales; our measurements (black filled circle) and the existing measurements in the literature (purple filled squares, ref. 11; red crosses, ref. 12) are presented at the same angular scales. Error bars are the 1σ uncertainties directly propagated to a r.m.s. fluctuation amplitude from the power spectrum errors. We do not show the measurements at 1.6 and 1.1 μm (ref. 10) as they do not probe fluctuations on scales greater than 2 arcmin on the sky due to the narrow field of view of the observations. The shaded regions are predictions for the IHL taking a variety of spectral energy distributions for the stripped stars (green), $z > 6$ galaxies (yellow) and low-redshift galaxies below the detection level of masking (blue).

fraction of the total luminosity of the cluster. We describe the intensity anisotropy power spectrum from the IHL by modifying the standard galaxy clustering predictions[22] to include a profile for the diffuse stars in haloes (see Supplementary Information section 8). If the clustering excess in near-infrared anisotropy power spectrum is due to IHL, then we find that measured anisotropies can be described with haloes in the mass range of 10^9 to 10^{12} solar masses ($M_\odot$). Averaged over this mass range, we find an IHL fraction relative to the total luminosity $f_{\rm IHL}$ of 0.07–0.2% at a 68% confidence level (Fig. 2). The implied fraction is consistent with the theoretical expectation that the IHL level is small for low-mass haloes, but differences also exist with current theory predictions[13,14], especially in terms of the power-law slope of the halo mass dependence.

If this new interpretation involving IHL is the correct description of measured infrared background anisotropies, we find that the IHL in all dark-matter haloes that we are probing contribute 0.75 ± 0.25 nW m^{-2} sr^{-1} to the total intensity at 3.6 μm. This intensity can be compared to the r.m.s. fluctuations of about 0.1 nW m^{-2} sr^{-1} at an angular scale of a few arcminutes (see Fig. 3). The IHL fluctuation signal varies spatially at a level of 10–15% of its integrated intensity and below 1% of the total background intensity of 13.3 ± 2.8 nW m^{-2} sr^{-1} at 3.6 μm (ref. 27). As the spectral energy distribution of IHL is mostly unknown, we make use of a variety of spectral energy distributions (SEDs) from B- to K-type stellar spectral templates and find an order of magnitude variation at wavelengths of ~1 μm (Fig. 3). In all these cases, we predict the existence of optical background light fluctuations. They will have a similar power spectrum shape and will be fully correlated with fluctuations at 3.6 μm. Furthermore, the near-infrared anisotropies we have measured should be correlated with the submillimetre anisotropies[28], especially if there is diffuse and extended dust associated with galaxies. These form future tests that can be used to improve our understanding of the content and nature of IHL in distant dark-matter haloes.

Received 5 June; accepted 15 August 2012.

1. Santos, M. R., Bromm, V. & Kamionkowski, M. The contribution of the first stars to the cosmic infrared background. *Mon. Not. R. Astron. Soc.* **336,** 1082–1092 (2002).
2. Salvaterra, R. & Ferrara, A. The imprint of the cosmic dark ages on the near-infrared background. *Mon. Not. R. Astron. Soc.* **339,** 973–982 (2003).
3. Cooray, A., Bock, J. J., Keating, B., Lange, A. E. & Matsumoto, T. First star signature in infrared background anisotropies. *Astrophys. J.* **606,** 611–624 (2004).
4. Kashlinsky, A., Arendt, R., Gardner, J. P., Mather, J. C. & Moseley, S. H. Detecting population III stars through observations of near-infrared cosmic infrared background anisotropies. *Astrophys. J.* **608,** 1–9 (2004).
5. Fernandez, E. R., Komatsu, E., Iliev, I. T. & Shapiro, P. R. The cosmic near-infrared background II: fluctuations. *Astrophys. J.* **710,** 1089–1110 (2010).
6. Chary, R., Cooray, A. & Sullivan, I. Contribution to unresolved infrared fluctuations from dwarf galaxies at redshifts of 2–3. *Astrophys. J.* **681,** 53–57 (2008).
7. Helgason, K., Ricotti, M. & Kashlinsky, A. Reconstructing the near-IR background fluctuations from known galaxy populations using multiband measurements of luminosity functions. *Astrophys. J.* **752,** 113 (2012).
8. Kashlinsky, A., Arendt, R. G., Mather, J. & Moseley, S. H. Tracing the first stars with fluctuations of the cosmic infrared background. *Nature* **438,** 45–50 (2005).
9. Cooray, A. *et al.* IR background anisotropies in Spitzer GOODS images and constraints on first galaxies. *Astrophys. J.* **659,** L91–L94 (2007).
10. Thompson, R., Eisenstein, D., Fan, X., Rieke, M. & Kennicutt, R. C. Evidence for a z 8 origin of the source-subtracted near-infrared background. *Astrophys. J.* **666,** 658–662 (2007).
11. Matsumoto, T. *et al.* AKARI observation of the fluctuation of the near-infrared background. *Astrophys. J.* **742,** 124 (2011).
12. Kashlinsky, A. *et al.* New measurements of the cosmic infrared background fluctuations in deep Spitzer/IRAC survey data and their cosmological implications. *Astrophys. J.* **753,** 63 (2012).
13. Purcell, C. W., Bullock, J. S. & Zentner, A. R. Shredded galaxies as the source of diffuse intrahalo light on varying scales. *Astrophys. J.* **666,** 20–33 (2007).
14. Purcell, C. W., Bullock, J. S. & Zentner, A. R. The metallicity of diffuse intrahalo light. *Mon. Not. R. Astron. Soc.* **391,** 550–558 (2008).
15. Conroy, C., Wechsler, R. H. & Kravtsov, A. V. The hierarchical build-up of massive galaxies and the intracluster light since z=1. *Astrophys. J.* **668,** 826–838 (2007).
16. Ashby, M. L. N. *et al.* The Spitzer Deep, Wide-field Survey. *Astrophys. J.* **701,** 428–453 (2009).
17. Arendt, R. G., Fixsen, D. J. & Moseley, S. H. Dithering strategies for efficient self-calibration of imaging arrays. *Astrophys. J.* **536,** 500–512 (2000).
18. Jannuzi, B. T. & Dey, A. in *Photometric Redshifts and the Detection of High Redshift Galaxies* (eds Weymann, R., Storrie-Lombardi, L., Sawicki, M. & Brunner, R.) 111–116 (ASP Conf. Ser. Vol. 191, Astron. Soc. Pacif., 1999).
19. Cooray, A., Gong, Y., Smidt, J. & Santos, M. G. The near-IR background intensity and anisotropies during the epoch of reionization. *Astrophys. J.* **756,** 92 (2012).
20. Fernandez, E. R., Iliev, I. T., Komatsu, E. & Shapiro, P. R. The cosmic near infrared background. III. Fluctuations, reionization, and the effects of minimum mass and self-regulation. *Astrophys. J.* **750,** 20 (2012).
21. Madau, P. & Silk, J. Population III and the near-infrared background excess. *Mon. Not. R. Astron. Soc.* **359,** L37–L41 (2005).
22. Cooray, A. & Sheth, R. Halo models of large scale structure. *Phys. Rep.* **372,** 1–129 (2002).
23. Tal, T.&. van Dokkum, P. The faint stellar halos of massive red galaxies from stacks of more than 42000 SDSS LRG images. *Astrophys. J.* **731,** 89 (2011).
24. Lin, Y. & Mohr, J. J. K-band properties of galaxy clusters and groups: brightest cluster galaxies and intracluster light. *Astrophys. J.* **617,** 879–895 (2004).
25. Rudick, C. S., Mihos, J. C., Frey, L. H. & McBride, C. K. Tidal streams of intracluster light. *Astrophys. J.* **699,** 1518–1529 (2009).
26. Gonzalez, A. H., Zabludoff, A. I. & Zaritsky, D. Intracluster light in nearby galaxy clusters: relationship to the halos of brightest cluster galaxies. *Astrophys. J.* **618,** 195–213 (2005).
27. Levenson, L. R., Wright, E. L. & Johnson, B. D. DIRBE minus 2MASS: confirming the CIRB in 40 new regions at 2.2 and 3.5 microns. *Astrophys. J.* **666,** 34–44 (2007).
28. Amblard, A. *et al.* Submillimetre galaxies reside in dark matter haloes with masses greater than 3×10^{11} solar masses. *Nature* **470,** 510–512 (2011).
29. Carollo, D. *et al.* Structure and kinematics of the stellar halos and thick disks of the Milky Way based on calibration stars from Sloan Digital Sky Survey DR7. *Astrophys. J.* **712,** 692–727 (2010).
30. Courteau, S. *et al.* The luminosity profile and structural parameters of the Andromeda Galaxy. *Astrophys. J.* **739,** 20 (2011).

Supplementary Information is available in the online version of the paper.

Acknowledgements We acknowledge support from NSF CAREER (to A.C.), NASA ADAP and an award from JPL/Caltech. We thank R. Arendt for sharing his IRAC self-calibration code. We thank J. Bock and M. Zemcov for their contributions to the SDWFS project. This work is based on observations made with the Spitzer Space Telescope. This work also made use of data products provided by the NOAO Deep Wide-Field Survey. A.C. thanks the Aspen Center for Physics for hospitality.

Author Contributions A.C. planned the study, developed the IHL model, supervised the research work of J.S., F.D.B., C.C.F. and Y.G., and wrote the draft version of this paper. J.S. and C.C.F. performed the power spectrum measurements and F.D.B. interpreted those measurements with a halo model for the IHL. Y.G. developed a model for the high-redshift galaxies. All other co-authors contributed extensively and equally by their varied contributions to the SDWFS project (led by D.S. as the Principal Investigator), planning of SDWFS observations, analysis of SDWFS data, and by commenting on this manuscript as part of an internal review process.

Author Information Reprints and permissions information is available at www.nature.com/reprints. The authors declare no competing financial interests. Readers are welcome to comment on the online version of the paper. Correspondence and requests for materials should be addressed to A.C. (acooray@uci.edu).